
DIAGNOSIS DRIVEN ANOMALY DETECTION FOR CPS

A PREPRINT

✉ **Henrik S. Steude**

Institute of Automation Technology
Helmut Schmidt University
Hamburg, Germany
henrik.steude@hsu-hh.de

✉ **Lukas Moddemann**

Institute of Automation Technology
Helmut Schmidt University
Hamburg, Germany
lukas.moddemann@hsu-hh.de

✉ **Alexander Diedrich**

Institute of Automation Technology
Helmut Schmidt University
Hamburg, Germany
alexander.diedrich@hsu-hh.de

✉ **Jonas Ehrhardt**

Institute of Automation Technology
Helmut Schmidt University
Hamburg, Germany
jonas.ehrhardt@hsu-hh.de

✉ **Oliver Niggemann**

Institute of Automation Technology
Helmut Schmidt University
Hamburg, Germany
oliver.niggemann@hsu-hh.de

November 28, 2023

ABSTRACT

In Cyber-Physical Systems (CPS) research, anomaly detection—detecting abnormal behavior—and diagnosis—identifying the underlying root cause—are often treated as distinct, isolated tasks. However, diagnosis algorithms require symptoms, i.e. temporally and spatially isolated anomalies, as input. Thus, anomaly detection and diagnosis must be developed together to provide a holistic solution for diagnosis in CPS. We therefore propose a method for utilizing deep learning-based anomaly detection to generate inputs for Consistency-Based Diagnosis (CBD). We evaluate our approach on a simulated and a real-world CPS dataset, where our model demonstrates strong performance relative to other state-of-the-art models.

Keywords Machine Learning, Anomaly Detection, Diagnosis, Cyber-Physical Systems

1 Introduction

Diagnosing system failures, a process that identifies the root causes of malfunctions, is a critical task in many Cyber-Physical Systems (CPS) applications. The growing complexity of CPS has made it increasingly important to develop diagnostic approaches to ensure their robustness and reliability. Consistency-Based Diagnosis (CBD) has become the state-of-the-art for complex CPS when limited or no information about possible faults is available [Reiter, 1987, Diedrich and Niggemann, 2022].

CBD requires models that represent the normal working behavior of the CPS, typically formulated using propositional logic, comprising symbols for individual components within the system. Furthermore, CBD needs discrete health states of the system’s components, known as observations. These health states are often generated through anomaly detection methods [Jung et al., 2018, 2016]. However, diagnosis and anomaly detection are often treated separately in the literature. Current research in anomaly detection for multivariate time series often employs deep learning methods to identify anomalies at the system level or for individual signals [Garg et al., 2022]. Conversely, the diagnostic literature

frequently assumes that labels for anomalies are readily available or can be detected through simple statistical methods [Diedrich and Niggemann, 2021].

Particularly for large and complex CPS, modeling in terms of CBD is a complex task on which the quality of the diagnostic system heavily depends [Diedrich et al., 2022]. The system can be modeled at different levels within the system hierarchy. The more detailed the description, the more expensive and error-prone the modeling process becomes. The ideal level of detail should be aligned with the maintenance strategy [Console et al., 1999].

To demonstrate the practical challenges, consider a CPS monitoring thousands of sensor signals. These signals can be mapped to a substantially smaller set of subsystems, usually less than a hundred. Having health states available at the subsystem level would greatly simplify the construction of a diagnostic model, such as those proposed by Bunte et al. [2019] or Diedrich and Niggemann [2022], as opposed to relying on health states for each sensor. Yet, as shown in Figure 1, these aggregated health states are neither readily available nor easy to infer.

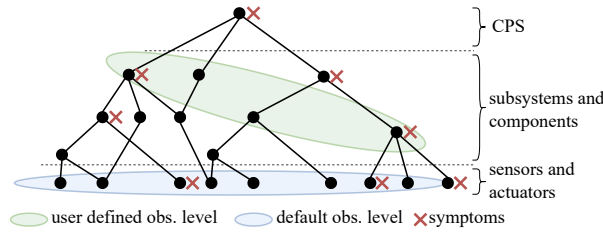


Figure 1: Exemplary system overview illustrating subsystems, components, sensors, actuators, and dependencies, with symptoms marked by red crosses.

In response to this challenge, we introduce an anomaly detection method tailored for identifying anomalies at the subsystem level, aligning with the needs of CBD’s system modeling. This method is specifically designed to manage the complexities of CPS datasets, which are often high-dimensional, time-dependent, and comprise a mix of data types [Niggemann et al., 2023].

The International Space Station’s (ISS) Columbus module serves as an example of a complex CPS. Developing diagnostic software based on telemetry data (see Figure 2) with over 20,000 signals has motivated the following research questions:

1. How effective are state-of-the-art deep learning approaches for anomaly detection at isolating symptoms at an aggregated subsystem level?
2. How can these methods be optimized for this specific challenge?

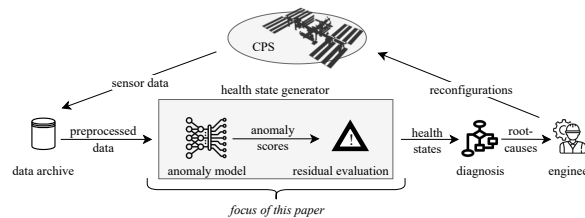


Figure 2: Example Use Case of the Columbus Module. This figure provides an overview of the high-level information flow in the ISS diagnosis system.

In this paper, we assume that the diagnosis model of the CPS, along with the mapping from signals to subsystems, is given as input. The paper’s focus lies on detecting symptoms, rather than on uncovering root causes. Previous work has shown how to use these health states to identify root causes Diedrich and Niggemann [2022].

Given this context, our paper makes two primary contributions: (i) We introduce a novel neural network (NN) architecture specifically designed to generate inputs for CBD algorithms by localizing symptoms within CPS data streams at the subsystem level. (ii) Through a simulated dataset, we highlight the limitations of current models in isolating symptoms at the subsystem level and demonstrate the superior performance of our approach. Furthermore, using the SWaT dataset [Goh et al., 2017], we show that our model’s overall anomaly detection capabilities are

competitive with other state-of-the-art models. The source code for our neural network architecture and the associated experiments is available at our GitHub repository¹.

2 Related Work

Based on the research questions developed in Section 1, two research areas are of particular interest to our investigation: diagnostics and anomaly detection for CPS.

The research field of model-based fault diagnosis goes back to the seminal work Reiter [1987]. Nowadays, many diagnosis algorithms exist [Rodler, 2022]. Physical system diagnosis has recently been addressed by Muškardin et al. [2020] and in the surveys by Dowdeswell et al. [2020] and Yucesan et al. [2021]. Jung et al. [2018] published an approach to combine Consistency-Based Diagnosis (CBD) with data-driven anomaly classifiers. Their aim was towards a novel technique for residual generation using one-class support vector machines, whose output was then diagnosed. In another work Lundgren and Jung [2022] present a data-driven approach for diagnosis compatible to CBD. In still other work, Jung [2022] has used a grey-box approach with neural networks and structural analysis to perform fault diagnosis. However, none of these approaches integrate anomaly detection with CBD on a logical knowledge base.

In the domain of anomaly detection for multivariate time series, deep learning methods have emerged as the state-of-the-art [Pang et al., 2021, Garg et al., 2022]. Broadly, these methods can be divided into reconstruction-based and prediction-based techniques. Within the group of prediction-based methods, modern network architectures such as Transformers [Chen et al., 2022a], TCNs [Cheng et al., 2019], and Graph Neural Networks [Deng and Hooi, 2021] are employed. Within reconstruction-based methods, similar approaches are combined with representation learning techniques like GANs [Li et al., 2019, Ciancarelli et al., 2023] and VAEs [Chen et al., 2022b, Lin et al., 2020]. Some of the mentioned methods have been explicitly evaluated in the context of CPS data, as demonstrated in Chen et al. [2022a] and Garg et al. [2022]. While some studies address anomaly detection in the context of diagnostics [Marino et al., 2021, Garg et al., 2022], none of these works to date have combined deep learning methods for multivariate time series with modern diagnostic techniques.

3 Solution

As outlined in Section 1, our objectives are to (i) identify symptoms (rather than root causes) in CPS data and (ii) localize them at the subsystem level. This section will formalize the problem and present our proposed solution.

3.1 Problem Specification

We assume that we have a set of subsystems denoted as S . Furthermore, we are provided with a mapping, referred to as the *subsystem-signals map*, which associates each subsystem with its corresponding set of CPS signals. Specifically, for each subsystem $s \in S$, this mapping defines the subset of signals $P_s \subseteq P$, where P is the set of all sensor signals, and P_s the set of signals associated with subsystem s . Let \mathbf{x}_p represent the time series of sensor $p \in P$, where each entry $x_p(t) \in \mathbb{R}$ holds the corresponding measurement value at timestamp t . For a simple example system, these quantities are visualized in Figure 3.

The anomaly detection system, which we call *symptom generator*, can be more formally described as a function G . This function takes the sensor readings from the most recent time window $\Delta t_w \in \mathbb{N}$, as input and returns a binary health state for each subsystem. Let the input \mathbf{X}_t be the matrix of sensor readings for the Δt_w most recent discrete time steps for all sensors, such that $\mathbf{X}_t \in \mathbb{R}^{\Delta t_w \times |P|}$. As output, G yields a vector $\mathbf{h}(t)$ where each element $h_p(t)$ indicates the health state of the p -th subsystem at time t :

$$\mathbf{h}(t) = G(\mathbf{X}_t)$$

with $h_p(t) \in \{0, 1\}$, where 0 signifies "OK" and 1 signifies "not OK". These states can be used to assign values to the *observations* used by Diedrich and Niggemann [2022].

3.2 Proposed NN architecture

In order to implement G we introduce a novel NN architecture, which leverages the β -Variational Autoencoder (VAE) [Higgins et al., 2017] framework and adapts the Temporal Convolutional Network (TCN) [Bai et al., 2018] for the encoder and decoder NNs. This makes our implementation similar to the TCN-AE introduced by Meng et al. [2020]. We further integrate prior knowledge of the CPS in the form of a *subsystem-signals map* into the network architecture.

¹<https://github.com/hsteude/diag-driven-ad-4-cps.git>

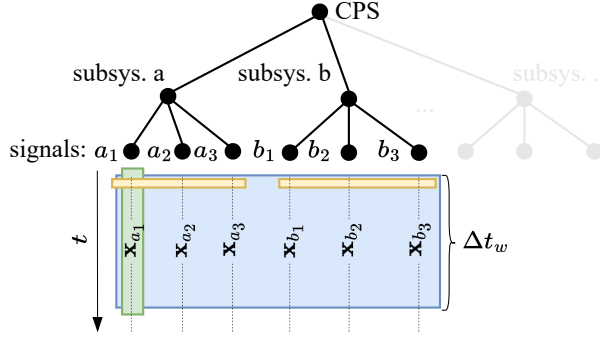


Figure 3: Visualization of a simple CPS example. The figure showcases two subsystems $S = \{a, b\}$, their signals $\{a_1, \dots, b_3\}$, and their time series $\{\mathbf{x}_{a_1}, \dots, \mathbf{x}_{b_3}\}$.

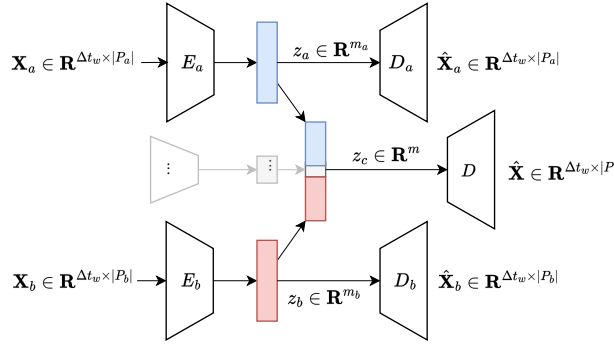


Figure 4: High-level model architecture. The visualizations of the latent space variables \mathbf{z}_a and \mathbf{z}_b , output by the encoders for subsystems a and b , are highlighted in blue and red, respectively. The encoders and decoders for additional subsystems are indicated in gray.

In the proposed architecture (visualized in Figure 4), the key innovation is the *composite latent space*. Signals from distinct subsystems, denoted by $i \in \{S\}$, are independently processed by dedicated encoder networks E_i . Each encoder produces a latent representation $\mathbf{z}_i \in \mathbb{R}^{m_i}$, where m_i represents the dimensionality of the latent space associated with subsystem i . These subsystem-specific latent vectors are then concatenated to form the *composite latent space* $\mathbf{z}_c \in \mathbb{R}^m$, satisfying $m = \sum m_i$ and ensuring that m is significantly less than the product of the time window length Δt_w and the number of signals $|P|$. The reconstruction of the full signal set P is performed by the decoder network D , which takes \mathbf{z}_c as input. This architectural design enforces an isolation constraint, preventing inter-subsystem information flow, thereby enhancing the fault isolation capability at the subsystem level. At the same time, the *composite latent space* \mathbf{z}_c ensures that cross-subsystem anomalies can be identified.

The second new component of our architecture is the structure of the individual encoder and decoder NNs. For simplicity, we describe this structure based on a simple encoder-decoder setup and omit the differentiation between individual subsystems and the corresponding indices. Figure 5 visualizes the architecture, which is representative of all encoders and decoders of the subsystems.

Our network architecture is built upon *residual blocks*, which consist of two convolutional layers with 'same' padding and equal dilation rates to maintain consistent temporal dimensions as well as skip connections. These blocks are organized into a *stacked dilated 1-D convolutional structure*, similar to TCNs. However, instead of using causal convolutions, our design employs non-causal ones, allowing for a full representation of the input sequence. Within these stacked blocks, channel dimensionality is reduced, followed by a max pooling operation that halves the time series length, thereby achieving temporal dimension reduction. Ultimately, a fully connected layer is utilized to generate the parameters for the posterior distribution $q(\mathbf{z}|\mathbf{X})$ from the output of the second max pooling layer. The latent variable \mathbf{z} sampled from this distribution is fed into the decoder D . The decoders echo the encoder's architecture, substituting max pooling with upsampling layers to reinstate the original time series dimension.

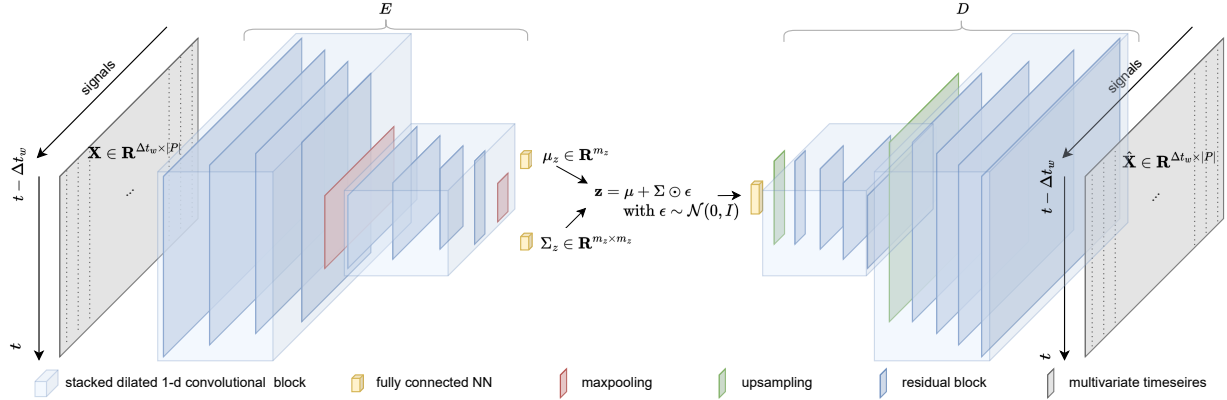


Figure 5: Schematic of our TCN-VAE architecture. This architecture is used within E_i and D_i as referenced in Figure 4

The loss function we use for adjusting the weights consists of three components: the mean squared error (MSE) for each individual decoder averaged across all decoders, the Kullback-Leibler (KL) divergence averaged across all individual posterior distributions relative to their respective priors, and the global MSE for the entire set of signals. Formally, the loss function is defined as follows:

$$\mathcal{L} = \frac{1}{|S|} \sum_{i=1}^{|S|} \left[\text{MSE}(\mathbf{X}_i, \hat{\mathbf{X}}_i) + \beta \text{KL}(p(\mathbf{z}_i) \| q(\mathbf{z}_i | \mathbf{X}_i)) \right] + \text{MSE}(\mathbf{X}, \hat{\mathbf{X}}) \quad (1)$$

where each \mathbf{X}_i holds the signals associated to the subsystem i in the *subsystem-signals map* and $\hat{\mathbf{X}}_i$ is the reconstruction i.e. the output of decoder i . $\beta \in \mathbb{R}$ is the regularization weight introduced in Higgins et al. [2017].

3.3 Residual evaluation

To generate the binary health states \mathbf{h}_t that our function G is designed to produce, we use the reconstructions $\hat{\mathbf{X}}_i$ for all $i \in S$ as well as $\hat{\mathbf{X}}$. This process involves employing various scoring and thresholding methods, as detailed by Garg et al. [2022], who discuss a range of implementations and their respective pros and cons. In our implementation, we use the reconstruction error from individual subsystems and the overall error across all signals as our scoring function, and we select the best F1-score method for thresholding, following the approaches presented in the cited work. Ultimately, the efficacy of the model depends on the difference in reconstruction error between an *OK* sample and a *not OK* sample. The larger this difference, the easier the binarization.

4 Experiment

Our main experiment aims to investigate how the *composite-latent-space* performs in comparison to other architectures. To our knowledge, there is no publicly available CPS dataset that contains symptom labels at the subsystem level, necessitating the use of a simulated dataset for this analysis. However, we were able to demonstrate the capability of our architecture to detect anomalies within the entire system in a secondary experiment by applying our model to the SWaT dataset [Goh et al., 2017]. With a composite F1 score of 0.52, it ranks among the best of the models benchmarked by Garg et al. [2022]. We do not further elaborate on this experiment here, as the focus of this paper is on symptom isolation at the subsystem level. For corresponding details, we refer to our code repository.

Dataset The simulation assumes a system structured as shown in Figure 3, comprising two subsystems $S = \{a, b\}$ and a total of six signals $P = \{a_1, a_2, \dots, b_3\}$. The signals a and b visualized at the top of Figure 6 can be thought of as steering signal for their subsystems. These causal signals are not included in the dataset, they are only used during data generation. The length of the high and low states of signal a is randomly sampled from a uniform distribution, ranging between 500 and 1000 timesteps. Signal b is a delayed version of signal a . Signals a_1, a_2 , and a_3 are derived from the causal signal a , with a_1 mirroring a , a_2 representing the response of a second-order dynamic system, and a_3 that of a first-order dynamic system. Signals b_1, b_2 , and b_3 are based on the causal signal b , where b_1 is signal b with added noise, and b_2 and b_3 are its low-pass and high-pass filtered versions, respectively.

Benchmark models We have selected four modeling approaches commonly utilized in practice as baselines:

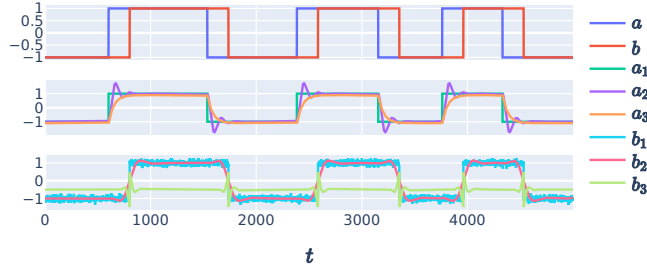


Figure 6: Healthy data sample (500 timestamps). Causal signals a and b (top) with derived signals a_1 to a_3 and b_1 to b_3 (middle and bottom), used for model training and validation.

1. A *vanilla TCN-VAE*, consisting of an extensive encoder and decoder that processes all signals from the CPS, reconstructing the input data (illustrated in blue in Figure 3). For the computation of the reconstruction error each subsystems, the average error of the signals associated with the subsystem is used.
2. A *univariate TCN-VAE* whose encoder and decoder also follow the architecture depicted in Figure 5, but models each signal in P independently (shown in green in Figure 3). The subsystem-specific reconstruction error is also derived by aggregating the errors of the corresponding signals.
3. A *Gaussian Mixture Model (GMM)* trained on individual time points, which only captures the data distributions at each timestamp. Here, a separate model is trained for each subsystem to derive a specific anomaly score (represented in yellow in Figure 3).

To ensure a fair comparison of the models’ performance, all models, with the exception of the GMM, share the same TCN-VAE architecture for their encoders and decoders. Additionally, the total number of parameters for all neural network models was kept in the same order of magnitude, approximately 500k. The total number of latent variables across all models was uniformly maintained at 12, and each model underwent independent hyperparameter tuning. With the optimal set of hyperparameters, the final models were trained using early stopping based on the validation loss.

Testing dataset The simulation described above represents the nominal operational condition, which we divide into training and validation sets. To assess the anomaly detection capabilities of the proposed model, we introduce four distinct fault scenarios into the dataset:

- Fault 1: The signal a_1 remains constant at a value of -1, simulating a stuck-at fault condition.
- Fault 2: An offset is introduced to signal b_3 , elevating its value by +1, reflecting a calibration or drift fault.
- Fault 3: A temporal shift is applied to all signals within subsystem b , mimicking a delay fault.
- Fault 4: The signals for both subsystems are modulated to operate at twice their normal frequency, representing a speed or performance anomaly.

The test set consists of 100 samples from each of the four distinct fault scenarios (1-4) and 400 samples from the healthy state, ensuring a balanced representation of labels. We utilized a binary labeling scheme, where 0 denotes the absence and 1 signifies the presence of faults within the respective subsystems and across the entire signal set, as outlined in Table 1.

Table 1: Label allocation in the test set.

Fault type	Subsys. a	Subsys. b	All signals
Healthy	0	0	0
Fault 1	1	0	1
Fault 2	0	1	1
Fault 3	0	0	1
Fault 4	1	1	1

Thresholds for anomaly detection in each model and subsystem were computed to optimize their respective F1 scores. The results are detailed in the subsequent section.

5 Results

The performance metrics from our experimental analysis are presented in Table 2. Our model demonstrates a consistent improvement in F1 scores across individual subsystems, highlighting its effectiveness in fault detection. For system-wide symptom identification, our model’s performance is comparable to that of the *Vanilla TCN-VAE*, as anticipated. The development focus of the *composite-latent-space* method was the improvement of symptom isolation at the subsystem level, rather than enhancing detection capabilities across the entire system.

Table 2: Evaluation Results of Models Across Different Subsystems.

Model	Subsys.	F1	Precision	Recall
GMM	a	0.436	0.982	0.28
Univar. TCN-VAE	a	0.662	1	0.495
Vanilla TCN-VAE	a	0.854	0.82	0.89
Our model	a	0.945	1	0.895
GMM	b	0.664	0.99	0.5
Univar. TCN-VAE	b	0.973	0.952	0.995
Vanilla TCN-VAE	b	0.772	0.636	0.98
Our model	b	0.998	0.995	1
GMM	all	0.811	1	0.682
Univar. TCN-VAE	all	0.675	0.516	0.978
Vanilla-TCN	all	0.941	0.989	0.898
Our model	all	0.948	0.997	0.902

For a more detailed view of the results, Figure 7 visualizes the distributions of reconstruction errors—or negative log likelihoods in the case of the GMM—for each model and fault scenario.

The rightmost column of the plot indicates that only the Vanilla TCN-VAE and our proposed model consistently differentiate most fault conditions from the healthy state.

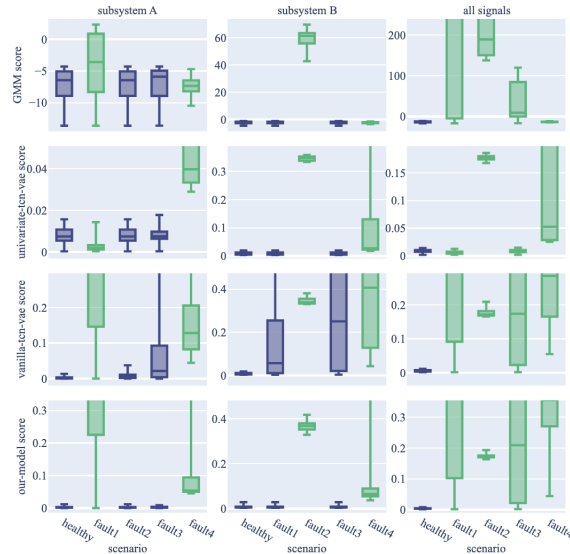


Figure 7: Distributions of model scores across different fault scenarios for subsystems *a*, *b*, and the aggregation of all signals. The green color indicates the presence of a symptom in the respective subsystem, while the blue color signifies the absence of a symptom.

The GMM does not exhibit a significant difference in the score distributions of fault 4 and the healthy scenarios. Similarly, the univariate model does not effectively distinguish between fault 1 and the healthy state. The GMM’s inability to recognize frequency changes in fault 4 stems from its focus on individual time points rather than on temporal patterns. Likewise, the univariate model lacks the capacity to detect temporal shifts between signals, as exemplified by fault 3.

However, the most notable observation concerns the Vanilla TCN-VAE model’s lack of precision within subsystems a and b . The reconstruction error distributions demonstrate that a symptom in subsystem a significantly increases the reconstruction error in subsystem b , and vice versa (faults 1 and 2).

This suggests that in standard reconstruction-based latent space models, the location of the greatest reconstruction error does not necessarily indicate the actual location of the symptom. The findings highlight that the *composite-latent-space* model effectively remedies this limitation.

6 Conclusion

In this study, we introduced a novel neural network architecture, termed the *composite-latent-space* architecture, designed to enhance symptom isolation capabilities within CPS at a user-defined level in the system hierarchy. The model was evaluated using a simulated dataset designed to represent various fault conditions.

Our results demonstrate that our model surpasses traditional models in isolating symptoms to specific subsystems. It is particularly interesting to note that larger holistic deep learning models, such as a sequence-to-sequence variational autoencoder without a specialized latent space structure, exhibited weak precision at the subsystem level.

While our model’s performance on the SWaT dataset illustrates its capability for system-wide anomaly detection, our focus is on the model’s superior symptom isolation at the subsystem level. This specificity in symptom identification is critical in the context of CBD, where binary health states for each subsystem are required as inputs.

For future work, we plan to evaluate the complete approach by diagnosing a comprehensive example system using subsystem health states generated by our proposed method. This will not only demonstrate the diagnostic capability at the macro level but also validate the practical applicability and effectiveness of our model in real-world CBD use cases.

References

- Raymond Reiter. A theory of diagnosis from first principles. *Artificial intelligence*, 32(1):57–95, 1987.
- Alexander Diedrich and Oliver Niggemann. On residual-based diagnosis of physical systems. *Engineering Applications of Artificial Intelligence*, 109:104636, 2022. ISSN 0952-1976. doi:<https://doi.org/10.1016/j.engappai.2021.104636>.
- Daniel Jung, Kok Yew Ng, Erik Frisk, and Mattias Krysander. Combining model-based diagnosis and data-driven anomaly classifiers for fault isolation. *Control Engineering Practice*, 80:146–156, 2018.
- Daniel Jung, Kok Yew Ng, Erik Frisk, and Mattias Krysander. A combined diagnosis system design using model-based and data-driven methods. In *Control and Fault-Tolerant Systems (SysTol), 2016 3rd Conference on*, pages 177–182. IEEE, 2016.
- Astha Garg, Wenyu Zhang, Jules Samaran, Ramasamy Savitha, and Chuan-Sheng Foo. An evaluation of anomaly detection and diagnosis in multivariate time series. *IEEE Trans Neural Netw Learn Syst*, PP, August 2022.
- Alexander Diedrich and Oliver Niggemann. Diagnosing systems through approximated information. In *Annual Conference of the PHM Society*, volume 13, 2021.
- Alexander Diedrich, Franziska Buchholz, and Oliver Niggemann. Learning a causal system description for diagnosing physical systems. In *Proceedings of the 33rd International Workshop on Principles of Diagnosis, Toulouse, France., 2022*.
- Luca Console, Oskar Dressler, et al. Model-based diagnosis in the real world: lessons learned and challenges remaining. In *IJCAI*, volume 99, pages 1393–1400. Citeseer, 1999.
- Andreas Bunte, Benno Stein, and Oliver Niggemann. Model-based diagnosis for cyber-physical production systems based on machine learning and residual-based diagnosis models. In *Proceedings of the AAAI Conference on Artificial Intelligence*, volume 33, pages 2727–2735, 2019.
- Oliver Niggemann, Bernd Zimmering, Henrik Sebasitan Steude, Jan Lukas Augustin, Alexander Windmann, and Samim Multaheb. Machine learning for cyber-physical systems. *Digital Transformation: Core Technologies and Emerging Topics from a Computer Science Perspective*, page 415, 2023.
- Jonathan Goh, Sridhar Adepur, Khurum Nazir Junejo, and Aditya Mathur. A dataset to support research in the design of secure water treatment systems. In *Critical Information Infrastructures Security*, pages 88–99. Springer International Publishing, 2017.
- Patrick Rodler. How should i compute my candidates? a taxonomy and classification of diagnosis computation algorithms. In *33rd International Workshop on Principle of Diagnosis – DX 2022, 2022*.

- Edi Muškardin, Ingo Pill, and Franz Wotawa. Catio-a framework for model-based diagnosis of cyber-physical systems. In *International Symposium on Methodologies for Intelligent Systems*, pages 267–276. Springer, 2020.
- Barry Dowdeswell, Roopak Sinha, and Stephen G MacDonell. Finding faults: A scoping study of fault diagnostics for industrial cyber-physical systems. *Journal of systems and software*, 168:110638, 2020.
- Yigit A Yucesan, Arinan Dourado, and Felipe AC Viana. A survey of modeling for prognosis and health management of industrial equipment. *Advanced Engineering Informatics*, 50:101404, 2021.
- Andreas Lundgren and Daniel Jung. Data-driven fault diagnosis analysis and open-set classification of time-series data. *Control Engineering Practice*, 121:105006, 2022.
- Daniel Jung. Automated design of grey-box recurrent neural networks for fault diagnosis using structural models and causal information. In *Learning for Dynamics and Control Conference*, pages 8–20. PMLR, 2022.
- Guansong Pang, Chunhua Shen, Longbing Cao, and Anton Van Den Hengel. Deep learning for anomaly detection: A review. *ACM Comput. Surv.*, 54(2):1–38, March 2021.
- Zekai Chen, Dingshuo Chen, Xiao Zhang, Zixuan Yuan, and Xiuzhen Cheng. Learning graph structures with transformer for multivariate Time-Series anomaly detection in IoT. *IEEE Internet of Things Journal*, 9(12):9179–9189, June 2022a.
- Yongliang Cheng, Yan Xu, Hong Zhong, and Yi Liu. HS-TCN: A semi-supervised hierarchical stacking temporal convolutional network for anomaly detection in IoT. In *2019 IEEE 38th International Performance Computing and Communications Conference (IPCCC)*, pages 1–7, October 2019.
- Ailin Deng and Bryan Hooi. Graph neural Network-Based anomaly detection in multivariate time series. *AAAI*, 35(5):4027–4035, May 2021.
- Dan Li, Dacheng Chen, Baihong Jin, Lei Shi, Jonathan Goh, and See-Kiong Ng. MAD-GAN: Multivariate anomaly detection for time series data with generative adversarial networks. In *Artificial Neural Networks and Machine Learning – ICANN 2019: Text and Time Series*, pages 703–716. Springer International Publishing, 2019.
- Carlo Ciancarelli, Giorgio De Magistris, Salvatore Cognetta, Daniele Appetito, Christian Napoli, and Daniele Nardi. A GAN approach for anomaly detection in spacecraft telemetries. In *17th International Conference on Soft Computing Models in Industrial and Environmental Applications (SOCO 2022)*, pages 393–402. Springer Nature Switzerland, 2023.
- Ningjiang Chen, Huan Tu, Xiaoyan Duan, Liangqing Hu, and Chengxiang Guo. Semisupervised anomaly detection of multivariate time series based on a variational autoencoder. *Appl. Intell.*, July 2022b.
- Shuyu Lin, Ronald Clark, Robert Birke, Sandro Schönborn, Niki Trigoni, and Stephen Roberts. Anomaly detection for time series using VAE-LSTM hybrid model. In *ICASSP 2020 - 2020 IEEE International Conference on Acoustics, Speech and Signal Processing (ICASSP)*, pages 4322–4326, May 2020.
- Daniel L Marino, Chathurika S Wickramasinghe, Billy Tsouvalas, Craig Rieger, and Milos Manic. Data-Driven correlation of cyber and physical anomalies for holistic system health monitoring. *IEEE Access*, 9:163138–163150, 2021.
- Irina Higgins, Loic Matthey, Arka Pal, Christopher Burgess, Xavier Glorot, Matthew Botvinick, Shakir Mohamed, and Alexander Lerchner. beta-vae: Learning basic visual concepts with a constrained variational framework. In *ICLR*, 2017.
- Shaojie Bai, J Zico Kolter, and Vladlen Koltun. An empirical evaluation of generic convolutional and recurrent networks for sequence modeling. [urlhttp://arxiv.org/abs/1803.01271v2](http://arxiv.org/abs/1803.01271v2), 2018.
- Chao Meng, Xue Song Jiang, Xiu Mei Wei, and Tao Wei. A Time Convolutional Network Based Outlier Detection for Multidimensional Time Series in Cyber-Physical-Social Systems. *IEEE Access*, 8:74933–74942, 2020. ISSN 2169-3536. doi:10.1109/ACCESS.2020.2988797.